



Estimation of hydrological drought recovery based on GRACE water storage deficit

Alka Singh^{1&2,*}, John T. Reager³, Ali Behrangi⁴

¹Universities Space Research Association, Columbia, MD, 21046, USA.

5 ²NASA Goddard Space Flight Center, Greenbelt, MD, 20771, USA.

³Jet Propulsion Laboratory, California Institute of Technology, Pasadena, CA, 91109, USA

⁴Department of hydrology and atmospheric sciences, The University of Arizona, Tucson, AZ, 85721 USA

Correspondence to: Alka Singh (alka.singh@nasa.gov; +1.301.286.6386)

10 **Abstract.** Drought is a natural climate extreme phenomenon that presents great challenges in forecasting and monitoring for
water management purposes. Previous studies have examined the use of Gravity Recovery and Climate Experiment (GRACE)
terrestrial water storage anomalies to measure the amount of water ‘missing’ from a drought-affected region, and other studies
have attempted statistical approaches to drought recovery forecasting based on joint probabilities of precipitation and soil
15 moisture. The goal of this study is to combine GRACE data with historical precipitation observations to quantify the amount
of precipitation required to achieve normal storage conditions in order to estimate a likely drought recovery time. First, linear
relationships between terrestrial water storage anomaly (TWSA) and cumulative precipitation anomaly are established across
a range of conditions. Then, historical precipitation data are statistically modeled to develop simplistic precipitation forecast
skill. Three different precipitation scenarios are simulated by using a standard deviation in climatology. Precipitation scenarios
are convolved with precipitation deficit estimates to calculate best-estimate of a drought recovery period. The results show
20 that in the regions of strong seasonal amplitude (like monsoon belt) drought continues even with the above-normal precipitation
until its wet season. Historical GRACE-observed drought recovery period is used to validate the approach. Estimated drought
for an example month demonstrated 80% similar recovery period as observed by the GRACE.

1 Introduction

Drought is a widespread recurring natural hazard with several direct and indirect impacts. Shortage of water in an ecosystem
25 not only reduces water availability for human consumption but also causes extensive flora and fauna mortality. Dryland, with
little vegetation on the surface, increases soil erosion, reduces water resilience time and enhances the possibility of forest fires,
leading to many indirect disasters. Big historical droughts have affected millions of lives and cost billions of dollars in the last
half a century. For example, the 1988 USA drought is estimated to cost \$40 billion, 1999 drought in Asia affected 60 million
people (Mishra and Singh, 2010). Severe water-crises can put society in turmoil and drive large-scale migrations particularly
30 in the developing parts of the world for example 2011 East African drought, 2018 dry corridors of central America.

There are different definitions of drought depending on the context, including agricultural (soil moisture deficit),
meteorological (precipitation deficit), and hydrological (streamflow/groundwater deficit) droughts (AghaKouchak, 2014;
Ahmadi et al., 2019; Behrangi et al., 2015b; Mishra and Singh, 2011). Furthermore, various drought indicators are developed
based on different hydrological parameters (soil moisture, precipitation, and runoff) or for different application areas, like the
35 Palmer drought severity index (PDSI) (Palmer, 1965), standardized precipitation index (SPI) (McKee et al., 1993),
standardized precipitation evaporation index (SPEI) (Vicente-Serrano et al., 2009), etc. They heavily rely on the accuracy of
meteorological inputs, hence become unreliable where ground observations are sparse (Zhao et al., 2017). Several drought
indicies are based on remote sensed products like Normalized differential vegetation index (NDVI) (Keshavarz et al., 2014),
Evaporation stress index (ESI) (Otkin et al., 2013), Soil moisture index (SMI) (Sridhar et al., 2008), Soil water deficit index
40 (SWDI) (Martínez-Fernández et al., 2015). However, use of a consistent drought metrics for various climatic regimes is
essential for global drought studies. A comprehensive study of severity of hydrological drought requires combining both



surface (snow and surface water), and subsurface (soil moisture and groundwater) information, which may be hard to obtain using in situ methods, especially for a large study region.

Gravity Recovery and Climate Experiment (GRACE) mission enables us to measure the integrated water storage variation in a system, which includes surface water, soil moisture, and groundwater. Many studies have used GRACE to described the process and monitoring of drought (Awange et al., 2016; Forootan et al., 2019; Sun et al., 2017; Thomas et al., 2014; Yirdaw et al., 2008; Zhang et al., 2015). Yirdaw et al. (2008) were foremost in exploring the potential of GRACE in the drought monitoring in the Canadian Prairie region. Houborg et al. (2012) developed GRACE-based drought indicator by assimilating terrestrial water storage (TWS) into Catchment Land Surface Model (CLSM) over North America. Thomas et al. (2014), for the first time, used GRACE terrestrial water storage anomaly (TWSA) as an independent global drought severity index by considering negative deviations from the monthly climatology of the time series as storage deficits. This method can improve the characterization of drought because it provides both the total amount of missing water from an ecosystem and also clearly identifies the beginning and the end of a drought, on a monthly timescale. The ultimate benefit of this approach is that by quantifying the amount of water required in storage for a region to return to historical average conditions, the method allows for the identification of an explicit hydrological drought recovery target. Furthermore, the GRACE-based drought index is independent of other drought indices and the have global spatial coverage. While an increasing number of case studies have used GRACE to characterize drought in different regions, for example, Amazon (Chen et al., 2009; Frappart et al., 2012), Texas (Long et al., 2013), China (Zhao et al., 2018), a global gridded assessment of direct application of GRACE on drought are still a few.

Traditional drought monitoring indices (eg. SPI, PDSI) have no information about the drought recovery period. Recovery time can be a critical metric of drought impact, in showing how long an ecosystem requires to revert to its pre-drought functional state (Schwalm et al., 2017). With the increasing frequency of drought, it is essential for an ecosystem to recover completely before the successive drought, otherwise repeated exposure to stress can degrade the ecosystem for a long-term. A tentative estimate of expected recovery can help water management authorities to regulate the water supply until a system recovers completely from drought stress. Previous studies have analyzed historical drought events and different predictors like teleconnections, local climate variables (temperature, precipitation) for drought prediction (Behrangi et al., 2015a; Maity et al., 2016; Otkin et al., 2015; Yuan et al., 2013) but not much work has been done on drought recovery analysis. Many studies have analyzed causes and pattern of onset and termination of drought (Dettinger, 2013; Maxwell et al., 2013; Mo, 2011; Seager et al., 2019) but did not dwell into statistical evolution of drought recovery. Hao et al., (2018) reviewed a different kind of droughts and its prediction methods based on statistical, dynamical, and hybrid methods. (Pan et al., 2013) were the first to develop a probabilistic drought recovery framework based on an ensemble forecast. They used a Copula model to establish a joint distribution between cumulative precipitation and a soil-moisture-based drought index to fine-tune their correlation structure. They demonstrated that drought recovery estimates typically have significant uncertainty and that a probabilistic approach can offer better information on realized drought risk. However, above-average rain in a given month may replenish surface water/soil moisture and support recovery in vegetation, but the true impact of drought continues until all hydrological compartments, including deep soil moisture and groundwater recover. This type of integrated drought onset and recovery phenomenon can only be estimated using integrated terrestrial water storage observations.

Here we explored drought recovery time at a 0.5-degree gridded framework. Building upon previous works, we apply GRACE-observed storage deficits as a drought indicator and provide different probabilistic scenarios for drought recovery based on historical precipitation analysis. Specifically, we estimate the required-precipitation to fill a storage deficit by deriving a linear relationship between precipitation and storage variability. Here, we focus on sub-decadal drought only within the GRACE period. Different precipitation scenarios are generated for precipitation inputs based on the distribution of historical observations. The required-precipitation estimates are validated by the duration of drought using GPCP and GRACE observations independently.



85 2 Data

2.1 GRACE

The GRACE mission operated from April 2002- June 2017 with a primary goal to track water redistribution on Earth and to improved our understanding of the global and regional water cycle. The GRACE-based TWSA includes integrated water mass changes in a vertical column which may consist of rivers, lakes, snow, ice, glaciers, soil moisture, permafrost, swamp, groundwater, etc. We downloaded the GRACE mascon (RL06) solutions from the Jet Propulsion Laboratory (JPL) website <https://grace.jpl.nasa.gov> (Wiese et al., 2018). The gravity field signals of the GRACE are pre-processed to monthly-gridded equivalent water height (EWH) variations by JPL (Watkins et al., 2015; Wiese et al., 2016). The mascon GRACE solutions are provided at 0.5-degree lon-lat grid, but they represent the 3x3 degree equal-area caps. Shape and size of the mascon caps vary with latitude. Therefore, the gridded mascon solutions are multiplied by a scaling factor grid
90 (https://grace.jpl.nasa.gov/data/get-data/jpl_global_mascons/), to improve the interpretation of signals at sub-mascon resolution. Since 2011, the GRACE dataset has data gaps of 1-2 months in every 5-6 months due to the aging batteries of the satellites. However, to compare precipitation and storage variability, a continuous monthly TWSA time-series is required. Therefore, the data gaps in the time-series are filled by cubic convolution interpolation.

2.2 GPCP

100 The latest global monthly precipitation data is obtained from the Global Precipitation Climatology Project (GPCP V2.3), from their website <https://www.esrl.noaa.gov/psd/> (Adler et al., 2003) for 1979-2017. It is a combined satellite-based product, adjusted by the rain gauge analysis. The downloaded 2.5-degree resolution data is re-gridded to 0.5 degrees to harmonize it with the grid resolution of the GRACE solutions.

The spatial resolution of the original GRACE solution (3-degree mascon) and GPCP (2.5-degree) are comparable. However,
105 as mascon size varies with latitude, therefore to improve the interpretation both datasets are brought to the 0.5-degree grid.

3 Methods

3.1 Storage deficit

It is useful to know the total amount of missing water from an ecosystem in order to characterize a drought so that an explicit target can be assumed that defines a drought recovery. Currently, global gridded total water storage variations can only be
110 obtained from GRACE TWSA. The TWSA is first smoothed by three months moving average filter, followed by the removal of a linear trend to reduce the impact of long-term signals in the storage. A linear trend in storage variability can be caused by other continuous/long term processes than just precipitation, like upstream water abstraction, groundwater pumping, increase/decrease in snowmelt, etc. The reduced TWSA is termed as dTWSA. The deviation of storage (dTWSA) from its normal water storage cycle (i.e., its historical climatology) can give an idea of the severity of drought phenomena. Here, we
115 define 'recovery' as a return to the climatological storage state for a given month. The climatology of the time series is estimated over the 15-year GRACE record (April 2002-March 2017) by averaging values from the same months of each year (i.e., all Januaries, all Februaries, so on). The negative residuals of the dTWSA from its climatology are considered as water storage 'deficit' in a grid cell (Thomas et al., 2014). If the duration of negative residuals is longer than three months, we designated it as a drought event. If recurring drought happens within a month gap (i.e., recovery shorter than one-month
120 duration), we considered it a continuation of the same drought. The green plot in Fig.1 shows the duration and severity of recurring drought in an example location in Australia (centered on 133.75°E 16.75°S). Using this approach, we produce a global gridded drought characteristics record, which includes the frequency, severity, and duration of drought, for the 2002-2017 period. For any instance and location, the state of drought and its length can be identified by quantifying the water storage



deficit from dTWSA. Eventually, recovery duration for each drought can also be observed, i.e., how long negative residuals
125 from climatology continued. For instance, Figure-1 shows three major droughts and their respective recovery periods (1.5, 1
and 0.5 years) for a sample location in Australia.

Figure 1

3.2 Estimation of the required-precipitation for storage deficit

The amount of required-precipitation to overcome a deficit is estimated using the association between precipitation and TWSA.
130 Monthly GPCP observations are first reduced by their mean for the April 2002 – March 2017 period (i.e., the 15-year GRACE
data record) to obtain precipitation anomaly. Then the relationship between precipitation and storage anomalies are derived.
For this, first, both variables are smoothed by a three-month moving average low pass filter to remove high-frequency noise.
Then, their linear trends are removed to reduce the impact of other processes like groundwater, upstream abstraction, glacier
melts, etc (as discussed above) and to focus our analysis on sub-decadal drought events within the GRACE period. The
135 smoothed and detrended precipitation anomaly is then integrated in time to obtain a cumulative detrended smoothed
precipitation anomaly (cdPA) and compared with the smoothed and detrended storage anomaly (dTWSA).

An ecosystem may behave differently under stress (a deficit period) than under an excess-water situation. In this study, the
storage (dTWSA) and precipitation (cdPA) linear relationship have been analyzed only during historical deficit periods as the
system behaves differently under stress (Famiglietti et al., 1998; Vereecken et al., 2007). Several researchers used rainfall-
140 runoff curve like soil conservation service curve number (SCS-CN) for the computation of surface runoff based on
precipitation with an assumption of stable relation between rainfall and abstraction (Mishra et al., 2006; Singh et al., 2015;
Verma et al., 2017). This study also assumes that precipitation intensity for a region does not change significantly over time,
consequently, the relationship between precipitation and storage variability can be considered stable.

Figure 2 shows the strength of this relationship by correlation coefficients in the top panel and linear regression coefficients
145 in the bottom panel. In addition to storage variability, precipitation is also lost in other hydrological processes like
evapotranspiration, runoff, etc. Therefore, for most of the regions, required precipitation is more than the amount of missing
water (i.e., regression coefficients greater than 1), except for the regions with frozen surfaces or weak precipitation-storage
coupling (non-red regions in Figure 2a). For example, in higher latitudes, mass loss observed by GRACE during spring
snowmelt is not directly linked to precipitation. Additionally, highly arid regions also have weak precipitation and storage
150 signals. Therefore, the proposed method is not suitable for regions with weak precipitation-storage coupling. These regions of
the weak association are identified based on regression coefficients below 1 (Figure 2b), as less than one or negative
relationship between storage variability and precipitation may describe a case in which storage variability is not linked to a
direct precipitation effect. Also, locations having less than five months of drought in 15 years are considered as regions of the
weak association because we don't have enough drought samples to derive their association. The regions of weak association,
155 (regression coefficients less than 1) are considered as unsuitable for the GRACE based recovery analysis and have been masked
out in this study.

Figure 2

Based on the derived linear relationship between cdPA and dTWSA (Figure 2, bottom plot), a required-precipitation is
estimated for each regional drought period. The method for the estimation of required-precipitation is shown in Figure 3 at an
160 example location (133.75°E 16.75°S) in Australia. The top panel shows an agreement between cdPA (black plot) and dTWSA
(red plot). In the bottom panel, an absolute required-precipitation (blue plot) is calculated by adding precipitation climatology
to the estimated surplus required-precipitation (magenta plot), to fill the storage deficit (green plot). Analogous to an
accounting methodology, this approach applies the assumption that generally more precipitation than usual (climatology) is
required to replenish the losses incurred during drought. The example location has a strong annual signal (5 - 150 mm, with
165 predominantly winter rain), which led to a relatively high ratio of required precipitation to the amount of missing water.



3.3 Historical Precipitation analysis

Historical precipitation data from GPCP (1979 to 2017) are statistically analyzed in order to create a simplistic precipitation forecast. Note that the motivation for providing a precipitation forecast here is not to present a state-of-the-art precipitation prediction, but to demonstrate the potential utility of the terrestrial water storage deficit in determining required precipitation and estimating a likely time to recovery. This methodology could be augmented with any type of more complex precipitation forecasting approaches.

3.3.1 Precipitation signal decomposition

Historical precipitation data is decomposed into a linear trend, as well as seasonal, inter-annual and sub-seasonal components in order to explore temporal variability. First, an annual signal/climatology (mean of each month, e.g., all January, February, etc.) and a linear trend are extracted from the original signal. They are directly used for signal reconstruction with the assumption that a similar long-period trend will continue. Then, the residual signal is filtered by a 12-month low-pass window to split it into a smooth inter-annual signal and a high-frequency sub-seasonal signal. The linear trend and inter-annual signal together are considered to contribute to long-term variability. The individual variance of the annual, long-term and sub-seasonal signals is normalized by their sum, in order to get their fractional contribution to local variability (Figure 4). This provides an overview of the relative importance and spatial distribution of these components in global temporal variability. As figure 4 shows, most regions are dominated by a seasonal cycle in precipitation.

Figure 4

3.3.2 Signal reconstruction and forecasting skill

Based on the above findings, we formulate a statistical model for hindcasting precipitation. The extracted annual signal and the linear trend by signal decomposition (section 3.3.1) are directly used for the precipitation reconstruction, with the assumption of the continuation of the similar variability. Further, interannual variability in the precipitation data is added by autoregression for 10-14 months depending on the length of significant autocorrelation. Finally, the sub-seasonal signal is added, which can only be reconstructed for 0-3 months due to the lack of significant temporal autocorrelation.

Figure 5 shows the precipitation hindcast for January 2016-December 2017 at an example location (56.25°W 27.75°S) in the La-Plata basin. Figure 5a shows that the estimated precipitation (red plot) compared to its climatology (blue plot) and GPCP observations (black plot) for the same duration. Figure 5b shows the reconstructed interannual precipitation by autoregression. The figure shows that interannual autoregression (blue plot) signals have a good association with the observed interannual signal (black plot) until the first 11 months. The sub-seasonal auto autoregression is significant only for two months in the example location. The final hindcast is an integration of a linear trend, climatology, sub-seasonal and interannual auto autoregression.

Figure 5

3.3.3 Hindcast evaluation

The statistically reconstructed global precipitation time series for two years (January 2016 - December 2017) is evaluated by GPCP observations using Nash-Sutcliffe efficiency (NSE). NSE illustrates the model efficiency over the mean, i.e., if Nash-Sutcliffe coefficients are zero or less than zero, then the model is equal or worst than the observational mean respectively. Figure 6 (red region) shows that the reconstructed full signal is in good agreement with GPCP observations. In these regions, fractional variability in the climatology and long-term signal are most robust (Figure 4a & 4b). Regions dominated by the high-frequency fractional variance (Figure 4c) are not well represented in our model (the white and blue area of Figure 6).

Figure 6



205 3.4 Probabilistic recovery

Precipitation is the major control on drought dynamics. Knowing the amount of precipitation required to overcome a drought (at any instance and any location globally), presents the opportunity for the estimation of a likely drought recovery period. We can apply a probabilistic approach by using the historical precipitation forecast model to simulate different precipitation scenarios based on the historical distribution of precipitation for each region. Here, we propose three precipitation scenarios:

210 1) normal precipitation (as described in section 3.3.2), 2) one standard deviation wetter than normal precipitation (wet year) and 3) three standard deviations wetter than normal precipitation (exceptionally wet year). The latter two scenarios are based on a standard deviation from the local precipitation climatology, to simulate average rainy and extremely rainy months, respectively. Again, we assume that in order to overcome a deficit due to drought, the ecosystem needs to receive a surplus of water that surpasses the climatological average. It follows that if drier than normal conditions were to persist indefinitely, then

215 a drought could theoretically go on forever. The climatological average is integrated with the estimated surplus required precipitation (Figure 3b, magenta plot) to obtain the absolute required precipitation (Figure 3b, blue plot). Whenever precipitation is more than the absolute required precipitation; the system advances in recovery to its pre-drought state. Based on this hypothesis, we simulated the three scenarios for how long any instance of drought will continue, given the expected three precipitation cases. Note that the scenarios suggest the needed recovery time for normal, wet, and exceptionally wet

220 years, hence providing a minimum baseline for the duration of drought recovery.

4 Results

4.1 Observed recovery time based on GRACE and GPCP observation

In this study, drought is defined by the negative deviation of TWSA from its record-length climatology. The observed recovery duration is measured directly from the storage deficit, as described previously (Figure 1, Thomas et al., 2014). For our

225 approach, we need to know when the observed precipitation is more than the absolute required precipitation (Section 3.2). Figure 7 shows the recovery estimation of all the droughts occurred during 2002-2017 at four random example locations: Northwest tropical Australia (123.25°E 17.75°S), Northeast Argentina in La-Plata basin (56.25°W and 27.75°S), North India in Ganges Basin (78.75°E and 27.75°N), North Brazil in Amazon basin (57.25°W and 2.25°S). Whenever the observed precipitation (Figure 7, red plot i.e. GPCP) is larger than the required precipitation (blue plot) for its respective month, the

230 drought should end. Ideally, GRACE should also observe it simultaneously.

Figure 7

In Figure 7, observed precipitation (red dashed line) and absolute required precipitation (blue line) are shown only during drought periods (green shaded area). The figure shows that the precipitation during a drought typically stays below its monthly required-precipitation until the end of the drought. In most cases, precipitation crossed the required-precipitation limit in

235 precisely the same month when GRACE observed the end of storage deficit. Even for the case of recurring droughts with two or more months gap, both methods observed the end of drought on approximately the same month. To examine our method in detail we randomly selected a drought month and validated our approach and estimated the recovery time based on different precipitation scenario in the following section.

4.2 Example of storage deficit and required precipitation

240 In this section, we discuss drought in an example month of January 2016. During the study period (2002-2017), the year 2015-2016 was the strongest El-Nino on record and many regions experienced some drought. Nevertheless, it is a random selection of the month for the demonstration of recovery analysis and can be applied to any other time window. Figure 8 shows the regions under drought in January 2016 (Figure 8a) and the estimated required-precipitation to overcome the drought (Figure 8b). All colors other than white in the figure are drought-affected regions within the region of strong precipitation-storage



245 relations (discussed in section 3.2). The color bar demonstrates the severity of the drought, i.e., the amount of missing water
(top panel) and the respective amount of required precipitation (bottom panel). Figure 8a shows the eastern Amazon, southern
Australia, south-east Africa, and north India were under severe drought in 2016.

Figure 8

4.2.1 Validation

250 To validate our approach, we compared recovery periods in Figure 9. The figure shows the recovery period from the January
2016 drought state, observed by GRACE (Figure 9a) and estimated recovery based on absolute required precipitation and
GPCP observations (Figure 9b). Figure 9c highlights the consistency in the estimated recovery period where one indicates 1–
2 months difference, 2 indicates 3–4 months difference, 3 indicates 5–8 months difference and 4 indicates 9+ months
difference. The blue area in the figure is the region with extremely different recovery estimates, which can be accounted to an
255 error in datasets. For the January 2016 drought, approximately 80% of the global land area demonstrated a similar recovery
period (+/- 1-2 months) to what was predicted (category 1 in Figure 9c).

Figure 9

4.2.2 Different precipitation scenario

This section demonstrates the probability of recovery duration in different precipitation scenarios. In the first section, we talk
260 about the expected recovery percentage within a month in three different precipitation scenarios. And in the second section,
we projected the duration needed to overcome the January 2016 drought within the study period (until March 2017).

4.2.2.1 The expected one-month recovery state

Spatiotemporal patterns of drought at the global scale are largely uncharacterized. Often, one-month of surplus precipitation
is not enough to fill the entire deficit. However, if it rains significantly above average immediately after/during the drought,
265 the recovery time decreases dramatically. We stimulated one-month (February 2016) recovery percentage for the January 2016
drought, given the three different precipitation scenarios (discussed in section 3.4). The surplus precipitation within a month
(February) is divided by the required estimated precipitation to calculated percentage recovery. In most of the drought-affected
regions, recovery percentage of our forecasted normal precipitation (Section 3.3.2) for February 2016 is more than the recovery
percentage of observed GPCP precipitation (Figure 8d). This indicates, February 2016 was drier than our estimated normal.
270 Most of the region recovered in extremely wet scenario (Figure 8c) within a month, except, regions dominated by summer
monsoon (Figure 8c, blue/cyan colored area) with less than 30 % recovery, as February is not a rainy season for this region.
This shows a case that regions with high amplitude seasonal cycles in precipitation mostly recover during their rainy season,
which varies globally.

Figure 8

4.2.2.2 Best estimated time for recovery

275 Recovery time varies from immediate (i.e., one month) to several years across different climate zones and depending on the
severity of the drought. Figure 10 shows the predicted recovery duration of the January 2016 drought state, which ranges from
a month (blue color) to not recoverable within the study period of 15 months (dark red color). Figure 10d shows the recovery
duration observed by GRACE, which is considered as truth. Figure 10a & 10b show that most of the region under severe
280 drought in 2016 did not recover with even one standard deviation wetter than normal precipitation and the drought in these
regions continued beyond a year. In the extremely wetter (three standard deviations) than normal situation (Figure 10c) most
of the regions recovered within 4-5 months, except for regions of most severe drought, such as the South East Amazon, and
Southern Africa. Even in the extremely wet scenario, the monsoon region (Figure 10c, cyan color) recovered only during their
rainy season (in 6-7 months from January 2016). This demonstrates that information on the state of precipitation compared to
285 its usual can provide an idea of the expected drought recovery duration provided we know the amount of precipitation required.



Figure 10

5 Discussion

Here we define drought using the observed storage deficit from GRACE TWSA, which is a 3-months or greater negative deviation from the historical, record-length climatology for each region, following Thomas et al. (2014). Generally, we considered this to be a better metric of integrated drought effects than a negative departure from climatology in precipitation or soil moisture because the former includes all components of the water cycle and represents the integrated state of the local the water budget closure, dS/dt . We observe that occasionally precipitation anomalies are depressed a couple of months before GRACE sees the beginning of drought onset because the net water mass balance can stay stable for some time by a compensating decrease in ET and runoff. Similarly, precipitation shows a positive deviation from climatology (i.e., excess precipitation) well before GRACE observes the end of the drought because of the time-lag to fill the rootzone soil moisture (Eltahir and Yeh, 1999). (Dettinger, 2013; Maxwell et al., 2013) also argued that drought onset is quicker than drought termination. Sometimes very heavy rain can quickly bring a region entirely out of a drought, but in many cases, continuous surplus precipitation is needed to bring the entire soil water column (i.e., from the surface to groundwater) to fully recover. Only GRACE can measure total variations in all of the hydrological compartments in a region.

The critical feature of the GRACE-based drought recovery framework is the estimation of required-precipitation to fill a storage deficit. Figure 2 shows that TWSA is closely associated with cumulative precipitation anomaly for most regions, except in deserts and high-latitudes. In large arid regions, monthly storage variability is significantly low due to low rainfall. In high-latitudes, seasonal water storage variability is mainly driven by temperature because of snow accumulation and melt. Typically in cold regions, winter snow accumulation and spring snowmelt drive increases and declines in TWSA, decoupling the storage variability from precipitation variability, which leads to a phase shift in their seasonality and weak correlation between them (Reager and Famiglietti, 2013). For these reasons, a storage-based drought recovery metric is not as capable in desert and high-latitude areas and have been masked out in the results section.

Variability in the historical precipitation data is analyzed by signal decomposition to develop a simple precipitation forecast model. Precipitation signals are hindcast by combining the climatology with the linear trend and an interannual signal estimated from autoregression. Figure 4 shows that in most regions seasonal variability is the strongest signal, except in big deserts, Eurasia and northwest America. These regions have high monthly sub-seasonal variability in precipitation which is hard to reconstruct. Additionally, due to the contribution of snowfall in higher latitudes and very low rainfall in deserts, bias correction in precipitation data are relatively less reliable. Consequently, we have less confidence in precipitation simulations in those regions (Figure 6).

In addition to the normal precipitation forecast, two more precipitation scenarios are simulated based on one and three standard deviations from the climatology, assuming that a system recovers from drought only when the precipitation is more than the usual (climatological) precipitation of the corresponding month. Figure 10 demonstrates percentage recovery given these three different precipitation scenarios. The figure shows that most regions show significant recovery within a month in three standard deviations wetter than normal scenario, except for regions which are not in their respective rainy season. As precipitation can be scarce in non-rainy-season months, even three standard deviations wetter than the historical average precipitation would not be a substantial amount of rain to replenish the water deficit in these periods. We further investigate the recovery duration based on different precipitation scenario (Figure 11) and find that under normal precipitation, most regions will not recover significantly within the study duration, but for three standard deviations wetter-than-normal rain, they recover within 3-4 months. However, for the regions with strong seasonal intensity of precipitation (monsoonal region), the figure showed recovery only during its rainy season (after 6-7 months) even in extreme wet scenario.



We validated our required precipitation estimates by comparing the recovery period observed by GRACE and estimated by our method on the GPCP observations (Figure 8) at different locations, which showed good concurrence. Also in Figure 11, the drought recovery duration for an example month of January 2016 demonstrated a good agreement between the observed recovery by GRACE and estimated recovery by GPCP for most of the regions (80% within +/- 1 month).

330 Knowing the present state of precipitation, i.e., how much surplus we have over usual climatology of a region can give an idea of expected recovery duration, provided we know the amount of precipitation needed to fill the deficit. With the improved precipitation forecasting skills, more accurate drought recovery estimates can be obtained. Nevertheless, the study demonstrates a case of application of GRACE for the estimation of required precipitation for drought recovery.

6 Conclusions

335 Increasing water-demand and future uncertainties in climate necessitate the assessment of the potential impact of drought and its expected recovery duration. The consequences of drought can be minimized through adaptation and risk management efforts, informed by the amount of missing water in a system and required-precipitation needed to bring it back to normal. Recurring droughts due to insufficient recovery can be minimized to a large extent by managing water resources wisely particularly during the deficit period until all of the hydrological components revert to the pre-drought state. The study
340 demonstrates the utility of GRACE terrestrial water storage anomalies (TWSA) in obtaining statistics of hydrologic drought, i.e., its recovery period and required precipitation to recover with sensitivity test to different precipitation scenarios. The benefits of the GRACE-based drought index for drought analysis are: 1) the independency from other drought indices and 2) the spatial coverage of the GRACE data (much of the globe). However, recovery analysis is limited to the area where linear-relationships between TWSA and cumulative precipitation anomaly exhibit strong linkages

345 The findings of this study are 1) the GRACE based drought index is valid to estimate the required precipitation for drought recovery and 2) the period of drought recovery depends on the intensity of precipitation i.e. in the dry season of the year drought continues even with above-normal precipitation. The recovery period estimated by our approach matches well with the recovery observed by GRACE for most regions (80%) for the demonstrated drought month. This approach can be extended with the availability of new GRACE follow-on (GRACE-FO) datasets, launched in May 2018. The proposed method and
350 analyses in this study are applicable to the development of operational drought monitoring system that can provide the actionable information for drought recovery given that the skillful precipitation prediction is available.

Funding: This research was funded by the GRACE science team meeting.

Acknowledgments: The research was carried out at the Jet Propulsion Laboratory, California Institute of Technology, under
355 a contract with the National Aeronautics and Space Administration (80NM0018D004).

Conflicts of Interest: The authors declare no conflict of interest.

Author Contributions: For this research article Dr. Singh has contributed in the data curation, formal analysis, writing and visualization. Dr. Reager has conceptualized, supervised and acquired funding to conduct this study. He has also helped in writing and editing the text. Dr. Behrangi has also contributed by supervision and funding acquisition.

360

References

Adler, R. F., Huffman, G. J., Chang, A., Ferraro, R., Xie, P.-P., Janowiak, J., Rudolf, B., Schneider, U., Curtis, S., Bolvin, D., Gruber, A., Susskind, J., Arkin, P. and Nelkin, E.: The Version-2 Global Precipitation Climatology Project (GPCP) Monthly Precipitation Analysis (1979–Present), *J. Hydrometeor.*, 4(6), 1147–1167, doi:10.1175/1525-7541(2003)004<1147:TVGPCP>2.0.CO;2, 2003.
365

AghaKouchak, A.: A baseline probabilistic drought forecasting framework using standardized soil moisture index: application to the 2012 United States drought, *Hydrol. Earth Syst. Sci.*, 18(7), 2485–2492, doi:10.5194/hess-18-2485-2014, 2014.



- 370 Ahmadi, B., Ahmadalipour, A. and Moradkhani, H.: Hydrological drought persistence and recovery over the CONUS: A multi-stage framework considering water quantity and quality, *Water Research*, 150, 97–110, doi:10.1016/j.watres.2018.11.052, 2019.
- Awange, J. L., Khandu, Schumacher, M., Forootan, E. and Heck, B.: Exploring hydro-meteorological drought patterns over the Greater Horn of Africa (1979–2014) using remote sensing and reanalysis products, *Advances in Water Resources*, 94, 45–59, doi:10.1016/j.advwatres.2016.04.005, 2016.
- 375 Behrangi, A., Nguyen, H. and Granger, S.: Probabilistic Seasonal Prediction of Meteorological Drought Using the Bootstrap and Multivariate Information, *J. Appl. Meteor. Climatol.*, 54(7), 1510–1522, doi:10.1175/JAMC-D-14-0162.1, 2015a.
- Behrangi, A., Loikith, P., Fetzer, E., Nguyen, H., Granger, S., Behrangi, A., Loikith, P. C., Fetzer, E. J., Nguyen, H. M. and Granger, S. L.: Utilizing Humidity and Temperature Data to Advance Monitoring and Prediction of Meteorological Drought, *Climate*, 3(4), 999–1017, doi:10.3390/cli3040999, 2015b.
- 380 Chen, J. L., Wilson, C. R., Tapley, B. D., Yang, Z. L. and Niu, G. Y.: 2005 drought event in the Amazon River basin as measured by GRACE and estimated by climate models, *J. Geophys. Res.*, 114(B5), B05404, doi:10.1029/2008JB006056, 2009.
- Dettinger, M. D.: Atmospheric Rivers as Drought Busters on the U.S. West Coast, *J. Hydrometeor.*, 14(6), 1721–1732, doi:10.1175/JHM-D-13-02.1, 2013.
- 385 Eltahir, E. A. B. and Yeh, P. J.-F.: On the asymmetric response of aquifer water level to floods and droughts in Illinois, *Water Resources Research*, 35(4), 1199–1217, doi:10.1029/1998WR900071, 1999.
- Famiglietti, J. S., Rudnicki, J. W. and Rodell, M.: Variability in surface moisture content along a hillslope transect: Rattlesnake Hill, Texas, *Journal of Hydrology*, 210(1), 259–281, doi:10.1016/S0022-1694(98)00187-5, 1998.
- 390 Forootan, E., Khaki, M., Schumacher, M., Wulfmeyer, V., Mehrnegar, N., van Dijk, A. I. J. M., Brocca, L., Farzaneh, S., Akinluyi, F., Ramillien, G., Shum, C. K., Awange, J. and Mostafaie, A.: Understanding the global hydrological droughts of 2003–2016 and their relationships with teleconnections, *Sci. Total Environ.*, 650(Pt 2), 2587–2604, doi:10.1016/j.scitotenv.2018.09.231, 2019.
- Frappart, F., Papa, F., Santos da Silva, J., Ramillien, G., Prigent, C., Seyler, F. and Calmant, S.: Surface freshwater storage and dynamics in the Amazon basin during the 2005 exceptional drought, *Environ. Res. Lett.*, 7(4), 044010, doi:10.1088/1748-9326/7/4/044010, 2012.
- 395 Hao, Z., Singh, V. P. and Xia, Y.: Seasonal Drought Prediction: Advances, Challenges, and Future Prospects, *Reviews of Geophysics*, 56(1), 108–141, doi:10.1002/2016RG000549, 2018.
- Houborg, R., Rodell, M., Li, B., Reichle, R. and Zaitchik, B. F.: Drought indicators based on model-assimilated Gravity Recovery and Climate Experiment (GRACE) terrestrial water storage observations: GRACE-BASED DROUGHT INDICATORS, *Water Resour. Res.*, 48(7), doi:10.1029/2011WR011291, 2012.
- 400 Keshavarz, M. R., Vazifedoust, M. and Alizadeh, A.: Drought monitoring using a Soil Wetness Deficit Index (SWDI) derived from MODIS satellite data, *Agricultural Water Management*, 132, 37–45, doi:10.1016/j.agwat.2013.10.004, 2014.
- Long, D., Scanlon, B. R., Longuevergne, L., Sun, A. Y., Fernando, D. N. and Save, H.: GRACE satellite monitoring of large depletion in water storage in response to the 2011 drought in Texas: GRACE-BASED DROUGHT MONITORING, *Geophys. Res. Lett.*, 40(13), 3395–3401, doi:10.1002/grl.50655, 2013.
- 405 Maity, R., Suman, M. and Verma, N. K.: Drought prediction using a wavelet based approach to model the temporal consequences of different types of droughts, *Journal of Hydrology*, 539, 417–428, doi:10.1016/j.jhydrol.2016.05.042, 2016.
- Martínez-Fernández, J., González-Zamora, A., Sánchez, N. and Gumuzzio, A.: A soil water based index as a suitable agricultural drought indicator, *Journal of Hydrology*, 522, 265–273, doi:10.1016/j.jhydrol.2014.12.051, 2015.
- 410 Maxwell, J. T., Ortegren, J. T., Knapp, P. A. and Soulé, P. T.: Tropical Cyclones and Drought Amelioration in the Gulf and Southeastern Coastal United States, *J. Climate*, 26(21), 8440–8452, doi:10.1175/JCLI-D-12-00824.1, 2013.
- McKee, T. B., Doesken, N. J. and Kleist, J.: The relationship of drought frequency and duration to time scales, *Meteor. Soc.*, 179–184, 1993.

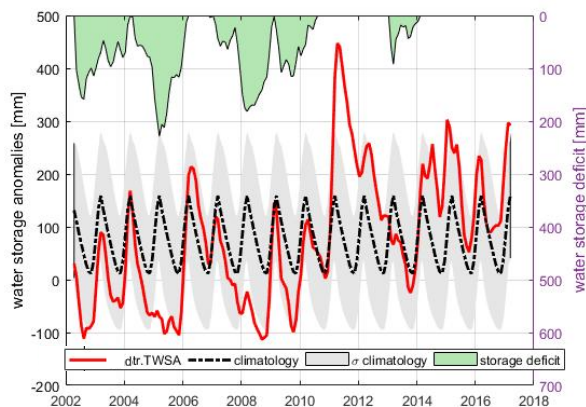


- Mishra, A. K. and Singh, V. P.: A review of drought concepts, *Journal of Hydrology*, 391(1), 202–216, doi:10.1016/j.jhydrol.2010.07.012, 2010.
- 415 Mishra, A. K. and Singh, V. P.: Drought modeling – A review, *Journal of Hydrology*, 403(1), 157–175, doi:10.1016/j.jhydrol.2011.03.049, 2011.
- Mishra, S. k., Sahu, R. k., Eldho, T. i. and Jain, M. k.: A generalized relation between initial abstraction and potential maximum retention in SCS-CN-based model, *International Journal of River Basin Management*, 4(4), 245–253, doi:10.1080/15715124.2006.9635294, 2006.
- 420 Mo, K. C.: Drought onset and recovery over the United States, *Journal of Geophysical Research: Atmospheres*, 116(D20), doi:10.1029/2011JD016168, 2011.
- Otkin, J. A., Anderson, M. C., Hain, C., Mladenova, I. E., Basara, J. B. and Svoboda, M.: Examining Rapid Onset Drought Development Using the Thermal Infrared–Based Evaporative Stress Index, *J. Hydrometeor.*, 14(4), 1057–1074, doi:10.1175/JHM-D-12-0144.1, 2013.
- 425 Otkin, J. A., Anderson, M. C., Hain, C. and Svoboda, M.: Using Temporal Changes in Drought Indices to Generate Probabilistic Drought Intensification Forecasts, *J. Hydrometeor.*, 16(1), 88–105, doi:10.1175/JHM-D-14-0064.1, 2015.
- Palmer, W. C.: Meteorological Drought, US Department of Commerce Weather Bureau, Washington DC, Research Paper No. 45 [online] Available from: <https://www.ncdc.noaa.gov/temp-and-precip/drought/docs/palmer.pdf> (Accessed 11 January 2018), 1965.
- 430 Pan, M., Yuan, X. and Wood, E. F.: A probabilistic framework for assessing drought recovery, *Geophysical Research Letters*, 40(14), 3637–3642, doi:10.1002/grl.50728, 2013.
- Reager, J. T. and Famiglietti, J. S.: Characteristic mega-basin water storage behavior using GRACE, *Water Resour Res*, 49(6), 3314–3329, doi:10.1002/wrcr.20264, 2013.
- 435 Schwalm, C. R., Anderegg, W. R. L., Michalak, A. M., Fisher, J. B., Biondi, F., Koch, G., Litvak, M., Ogle, K., Shaw, J. D., Wolf, A., Huntzinger, D. N., Schaefer, K., Cook, R., Wei, Y., Fang, Y., Hayes, D., Huang, M., Jain, A. and Tian, H.: Global patterns of drought recovery, *Nature*, 548(7666), 202–205, doi:10.1038/nature23021, 2017.
- Seager, R., Nakamura, J. and Ting, M.: Mechanisms of Seasonal Soil Moisture Drought Onset and Termination in the Southern Great Plains, *J. Hydrometeor.*, 20(4), 751–771, doi:10.1175/JHM-D-18-0191.1, 2019.
- 440 Singh, P. K., Mishra, S. K., Berndtsson, R., Jain, M. K. and Pandey, R. P.: Development of a Modified SMA Based MSCS-CN Model for Runoff Estimation, *Water Resour Manage*, 29(11), 4111–4127, doi:10.1007/s11269-015-1048-1, 2015.
- Sridhar, V., Hubbard, K. G., You, J. and Hunt, E. D.: Development of the Soil Moisture Index to Quantify Agricultural Drought and Its “User Friendliness” in Severity-Area-Duration Assessment, *J. Hydrometeor.*, 9(4), 660–676, doi:10.1175/2007JHM892.1, 2008.
- 445 Sun, A. Y., Scanlon, B. R., AghaKouchak, A. and Zhang, Z.: Using GRACE Satellite Gravimetry for Assessing Large-Scale Hydrologic Extremes, *Remote Sensing*, 9(12), 1287, doi:10.3390/rs9121287, 2017.
- Thomas, A. C., Reager, J. T., Famiglietti, J. S. and Rodell, M.: A GRACE-based water storage deficit approach for hydrological drought characterization, *Geophysical Research Letters*, 41(5), 1537–1545, doi:10.1002/2014GL059323, 2014.
- Vereecken, H., Kamai, T., Harter, T., Kasteel, R., Hopmans, J. and Vanderborght, J.: Explaining soil moisture variability as a function of mean soil moisture: A stochastic unsaturated flow perspective, *Geophysical Research Letters*, 34(22), doi:10.1029/2007GL031813, 2007.
- 450 Verma, S., Mishra, S. K., Singh, A., Singh, P. K. and Verma, R. K.: An enhanced SMA based SCS-CN inspired model for watershed runoff prediction, *Environ Earth Sci*, 76(21), 736, doi:10.1007/s12665-017-7062-2, 2017.
- Vicente-Serrano, S. M., Beguería, S. and López-Moreno, J. I.: A Multiscalar Drought Index Sensitive to Global Warming: The Standardized Precipitation Evapotranspiration Index, *J. Climate*, 23(7), 1696–1718, doi:10.1175/2009JCLI2909.1, 2009.
- 455 Watkins, M. M., Wiese, D. N., Yuan, D.-N., Boening, C. and Landerer, F. W.: Improved methods for observing Earth’s time variable mass distribution with GRACE using spherical cap mascons, *J. Geophys. Res. Solid Earth*, 120(4), 2014JB011547, doi:10.1002/2014JB011547, 2015.



- Wiese, D. N., Landerer, F. W. and Watkins, M. M.: Quantifying and reducing leakage errors in the JPL RL05M GRACE mascon solution, *Water Resour. Res.*, 52(9), 7490–7502, doi:10.1002/2016WR019344, 2016.
- 460 Wiese, D. N., Yuan, D.-N., Boening, C., Landerer, F. W. and Watkins, M. M.: JPL GRACE Mascon Ocean, Ice, and Hydrology Equivalent Water Height Release 06 Coastal Resolution Improvement (CRI) Filtered Version 1.0, , doi:10.5067/TEMSC-3MJC6, 2018.
- Yirdaw, S. Z., Snelgrove, K. R. and Agboma, C. O.: GRACE satellite observations of terrestrial moisture changes for drought characterization in the Canadian Prairie, *Journal of Hydrology*, 356(1–2), 84–92, doi:10.1016/j.jhydrol.2008.04.004, 2008.
- 465 Yuan, X., Wood, E. F., Chaney, N. W., Sheffield, J., Kam, J., Liang, M. and Guan, K.: Probabilistic Seasonal Forecasting of African Drought by Dynamical Models, *J. Hydrometeor.*, 14(6), 1706–1720, doi:10.1175/JHM-D-13-054.1, 2013.
- Zhang, D., Zhang, Q., Werner, A. D. and Liu, X.: GRACE-Based Hydrological Drought Evaluation of the Yangtze River Basin, China, *J. Hydrometeor.*, 17(3), 811–828, doi:10.1175/JHM-D-15-0084.1, 2015.
- 470 Zhao, C., Huang, Y., Li, Z. and Chen, M.: Drought Monitoring of Southwestern China Using Insufficient GRACE Data for the Long-Term Mean Reference Frame under Global Change, *J. Climate*, 31(17), 6897–6911, doi:10.1175/JCLI-D-17-0869.1, 2018.
- Zhao, M., A, G., Velicogna, I. and Kimball, J. S.: A Global Gridded Dataset of GRACE Drought Severity Index for 2002–14: Comparison with PDSI and SPEI and a Case Study of the Australia Millennium Drought, *J. Hydrometeor.*, 18(8), 2117–2129, doi:10.1175/JHM-D-16-0182.1, 2017.

475

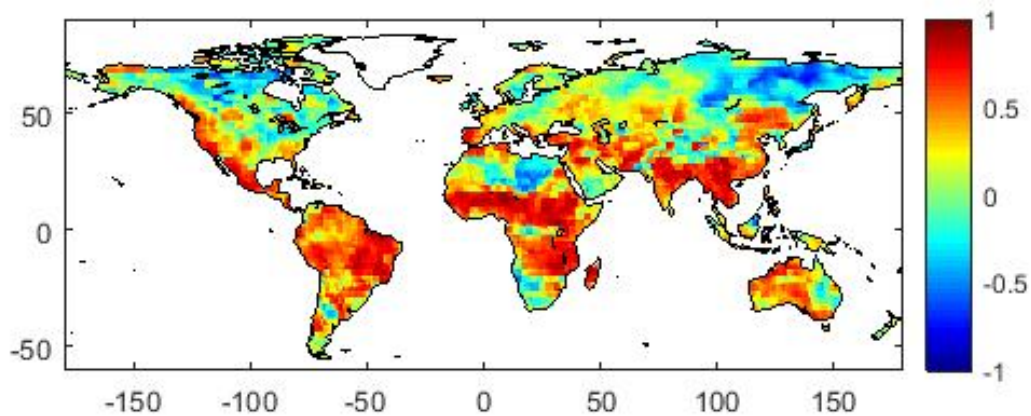


480

Figure 1: Water storage deficit from GRACE: The smoothed and detrended TWSA (dTWSA in red plot) is reduced by its climatology (black plot), to estimate deviation from the climatology. The negative residuals from the climatology are plotted on the upper axis as a green shaded area and scaled on the right side. The grey shade indicates ± 1 standard deviation of the climatology.



a) Correlation coefficients



b) Regression coefficients

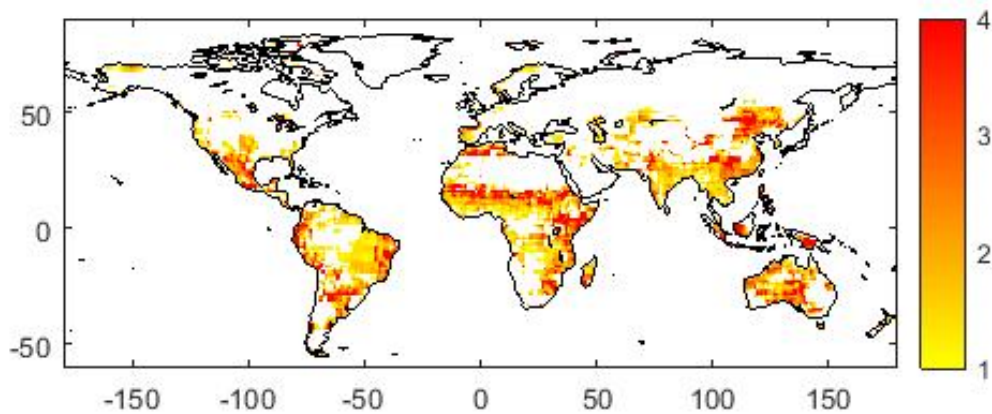


Figure 2: a) Correlation coefficients and, b) regression coefficients between cumulative detrended precipitation anomalies (cdPA) and detrended terrestrial water storage anomaly (dTWSA).

485

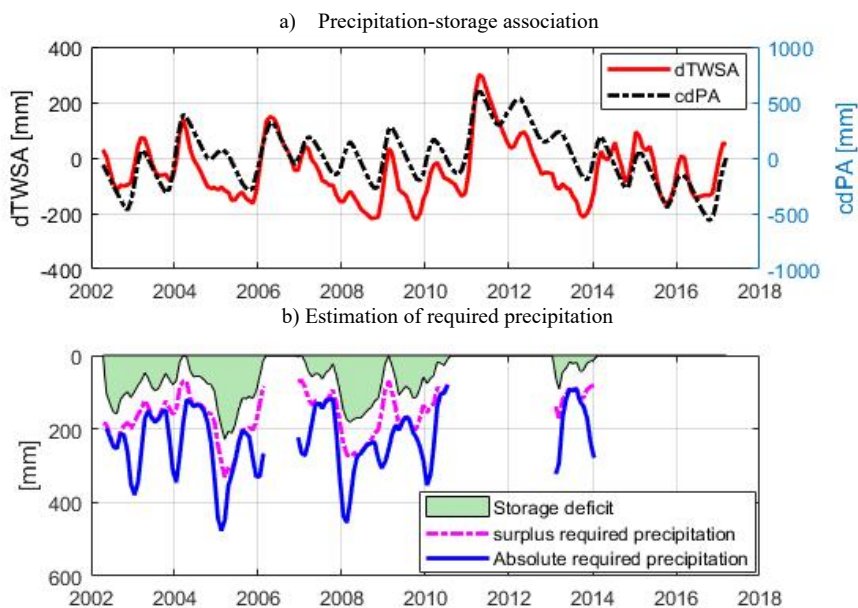


Figure 3: Estimation of the required-precipitation at an example location. a) Cumulative detrended precipitation anomaly (cdPA) compared with the detrended storage anomaly (dTWSA). b) Surplus required-precipitation is estimated (magenta plot) from the linear relationship between dTWSA and cdPA, to fill the storage deficit (green plot). Then precipitation climatology is added to obtain absolute required-precipitation (blue plot).

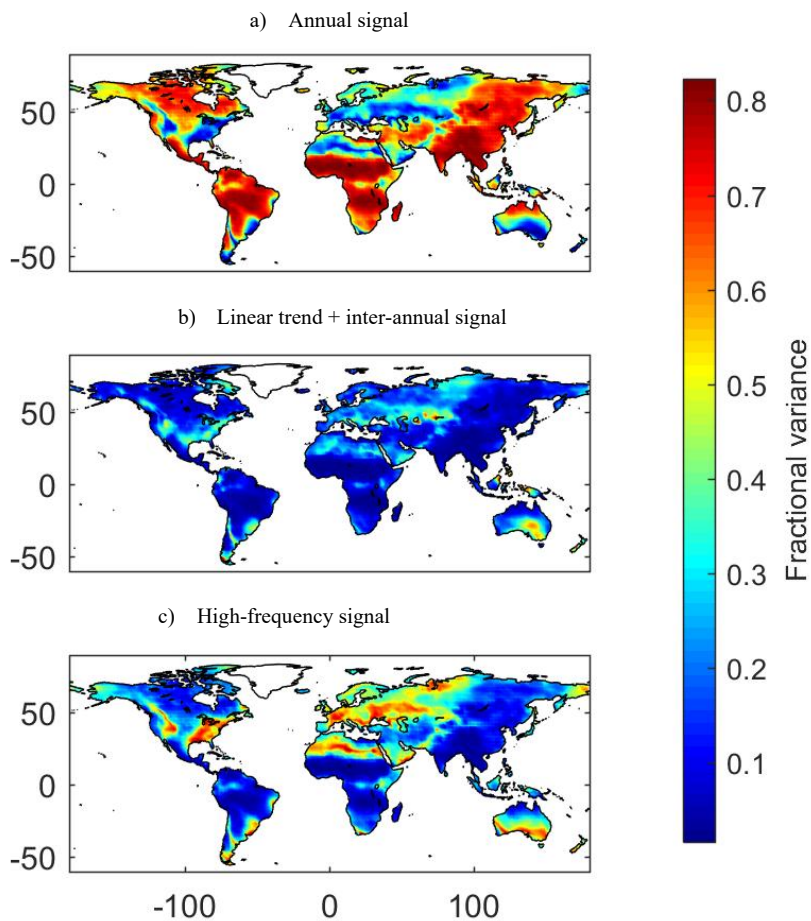


Figure 4: Fractional variance of the decomposed precipitation signal. a) Annual signal. b) long-term signal. c) sub-seasonal signal

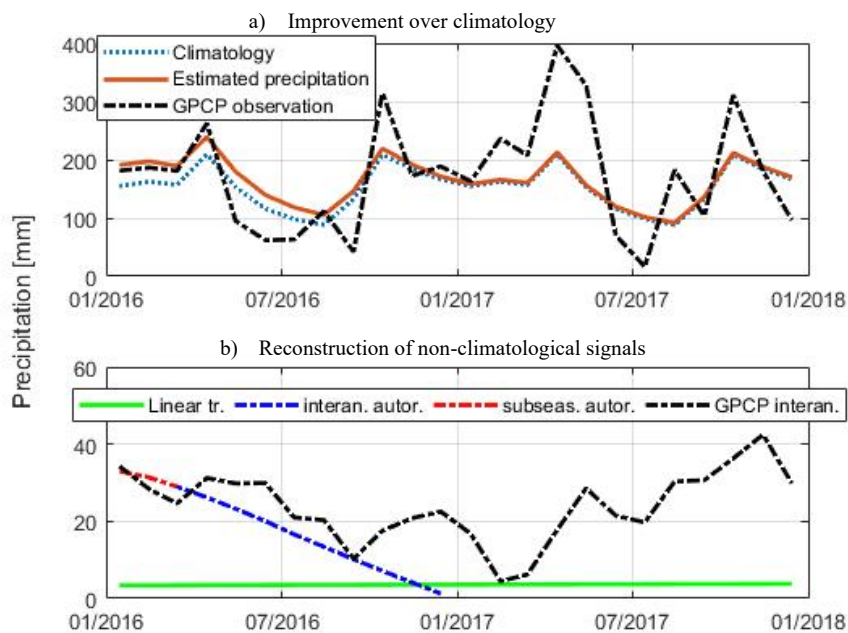


Figure 5: Reconstruction of precipitation signal for 2016-2017. a) The reconstructed signal compared with GPCP observations and its climatology. b) The reconstruction of a long-term secular signal from the linear trend, and inter-annual and sub-seasonal autoregression, compared to GPCP interannual signal.

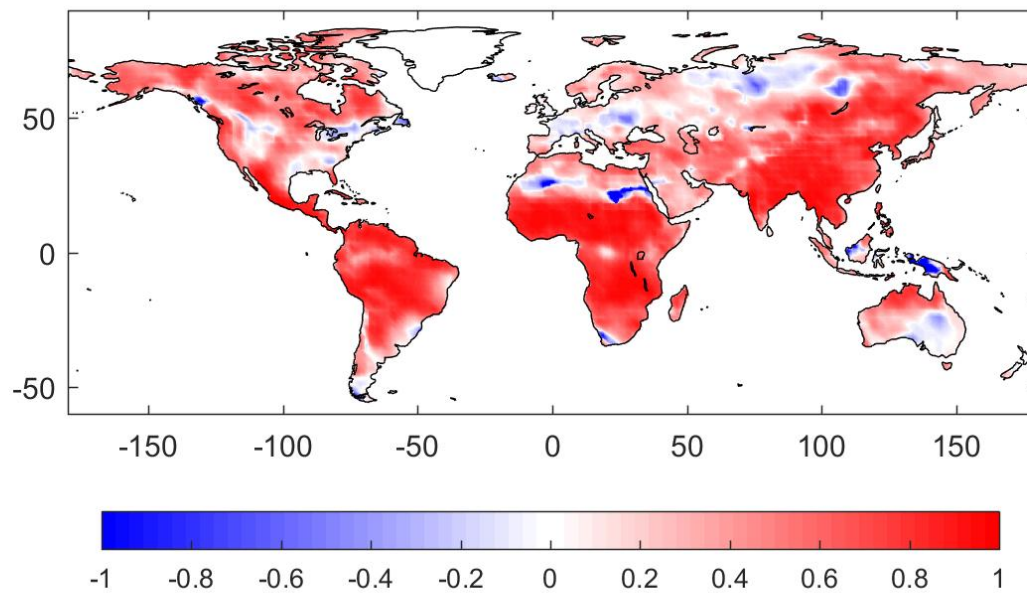


Figure 6: Nash-Sutcliffe coefficients for 2016-17 precipitation hindcasting.

490

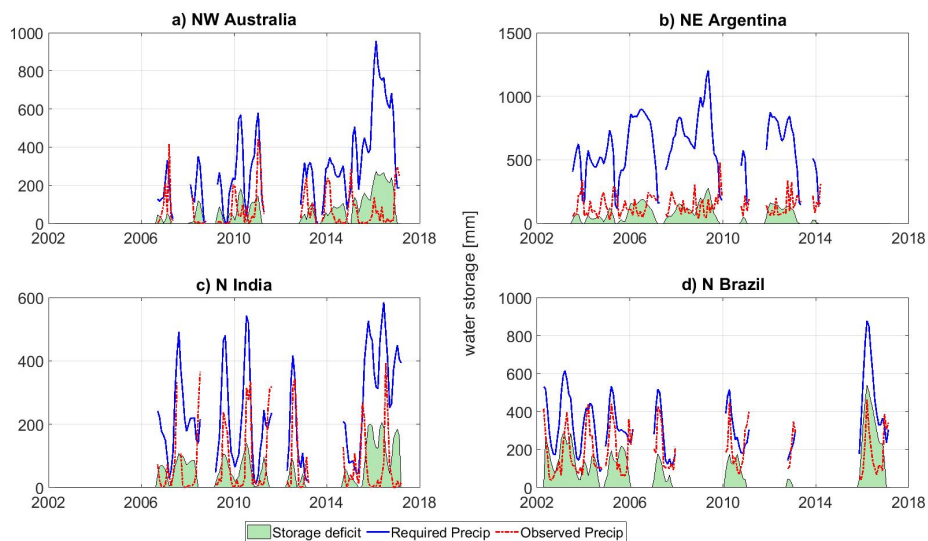


Figure 7 Validation of the required precipitation estimate by drought recovery estimates at example locations. The different instances of drought show that drought ends (from the perspective of TWSA) whenever observed precipitation (red plot) exceeds the required-precipitation (blue plot).

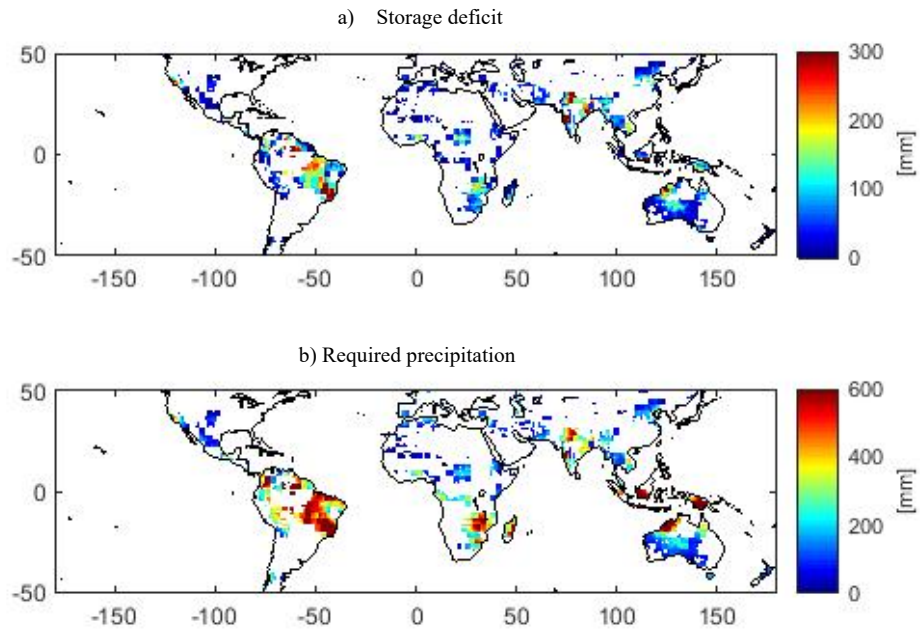


Figure 8: a) Storage deficit in an example month (January 2016). b) the amount of required-precipitation to fill the deficit.

495

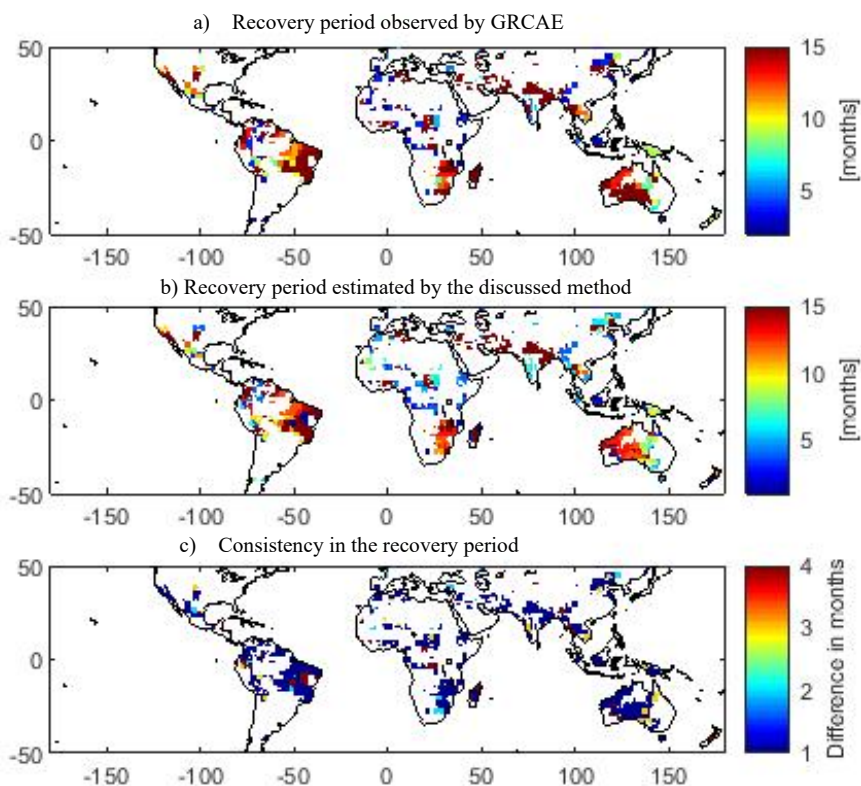


Figure 9: Validation of the estimated required-precipitation by the recovery duration from January 2016 drought observed from: a) GRACE and b) estimated by the discussed method using GRACE and GPCP observations (middle panel). c) consistency in the observed recovery duration by GRACE and GPCP (1 = 1-2 months difference, 2 = 3-4 months difference, 3 = 5-8 months difference and 4 = 9+ months difference).

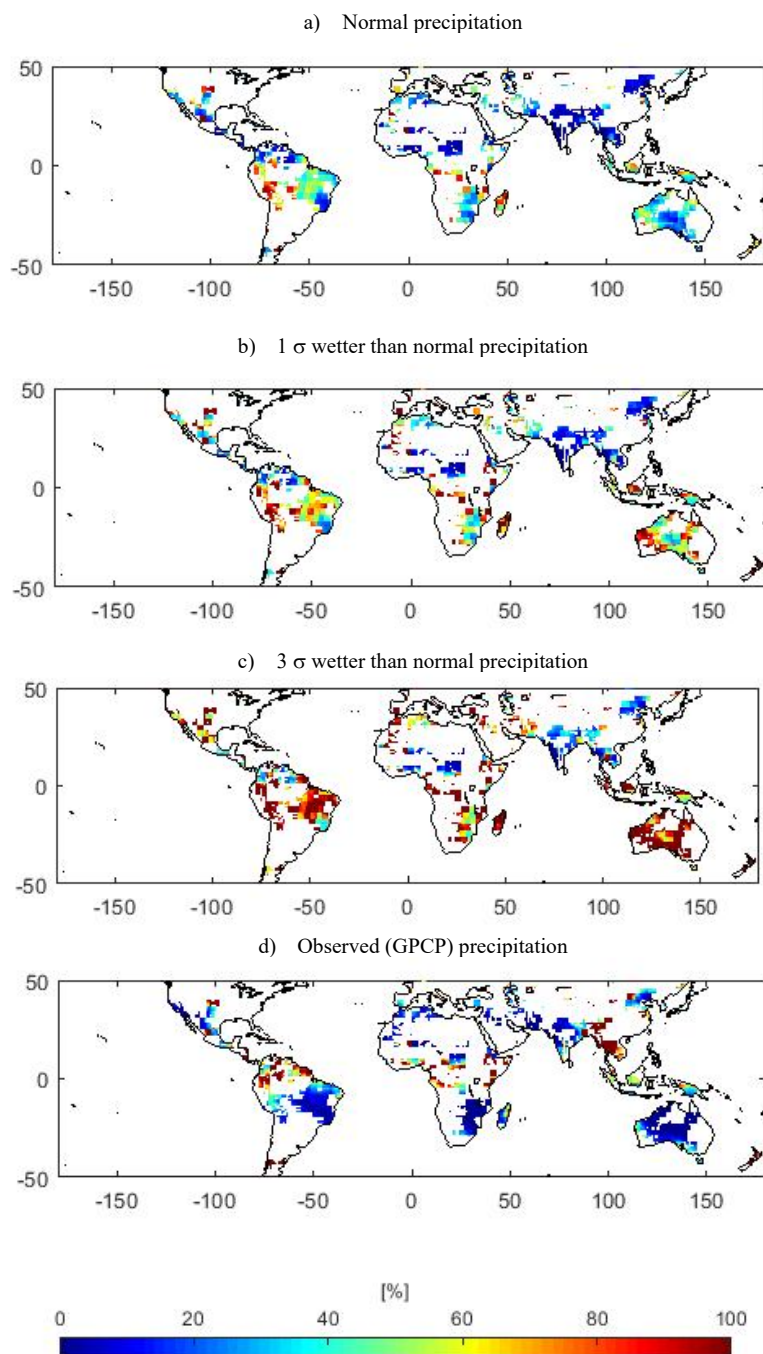


Figure 10: Expected percent recovery in a month given the three different precipitation scenarios and the observed GPCP precipitation.



500

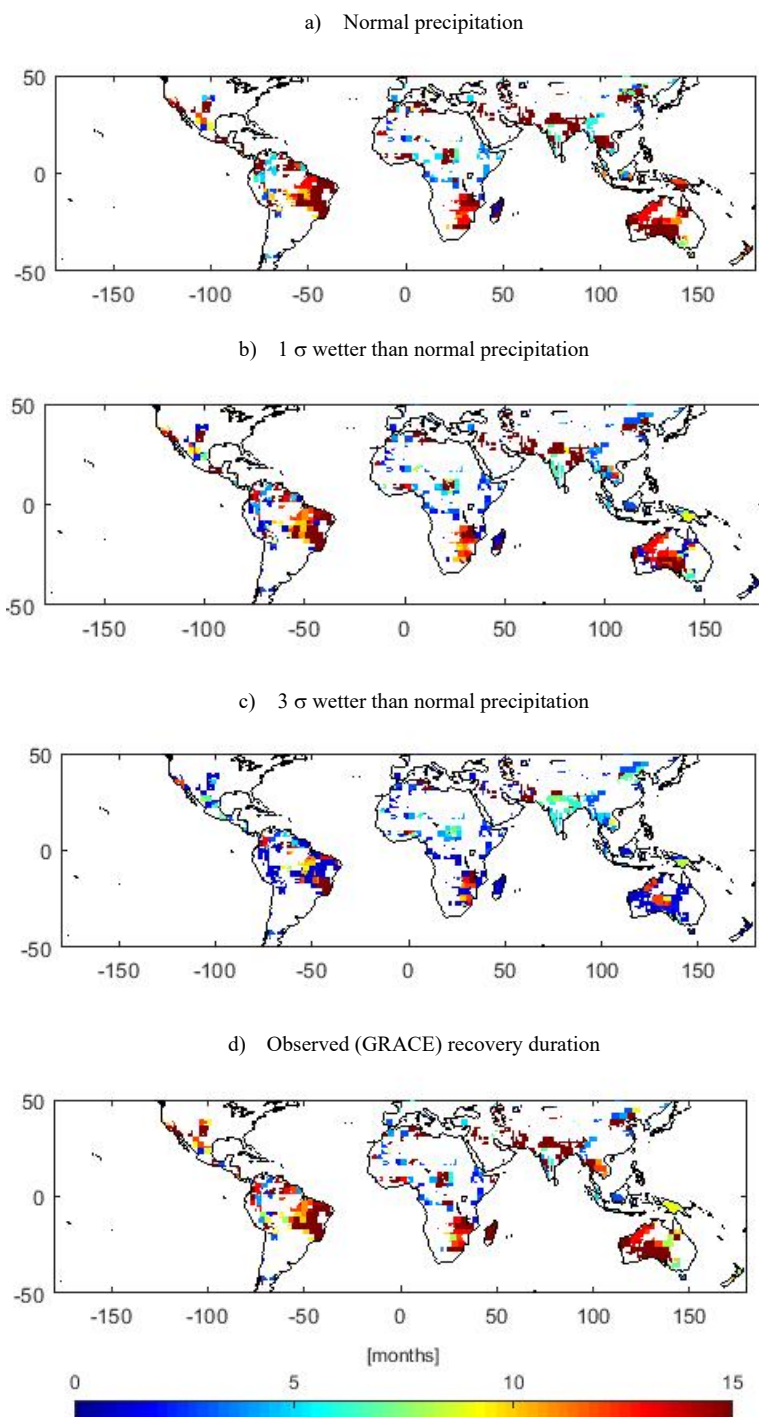


Figure 11: Duration of drought recovery, from January 2016, given the three different precipitation scenario and as observed by GRACE.